River Flow 2010 - Dittrich, Koll, Aberle & Geisenhainer (eds) - © 2010 Bundesanstalt für Wasserbau ISBN 978-3-939230-00-7

Validation of a non-linear reduced hydrodynamic model for curved open-channel flow

W. Ottevanger & W. S. J. Uijttewaal
Department of Civil Engineering and Geosciences, Delft University of Technology, The Netherlands

K. Blanckaert
ICARE-ENAC, Ecole Polytechnique Fédérale, Lausanne, Switzerland
Department of Civil Engineering and Geosciences, Delft University of Technology, The Netherlands
Institute of Freshwater Ecology and Inland Fisheries, Berlin, Germany

ABSTRACT: The flow through meander bends is inherently three dimensional and may be characterized by primary flow in streamwise direction and secondary flow in transverse direction. Although, three dimensional simulations of meander bends are feasible for laboratory scale experiments, temporal and spatial scales of naturally occurring meandering rivers are much larger than those found in laboratory experiments. Therefore, computationally less expensive (reduced) flow models are necessary. Reduced hydrodynamic models are depth-integrated models and therefore require a closure model to resolve the effect of secondary flow. At present, most reduced flow models are linear as they neglect the feedback between the primary and secondary flow, which limits their validity to mild curvature. A non-linear reduced flow model, including this feedback, is compared to experimental data from the laboratory and the field which are both sharply and moderately curved. The model predictions compare well to the global flow structure in the high curvature Kinoshita flume and the moderate curvature Tollense River bend (with extra complicating factors of vegetation and horizontal recirculation zones). A linear model is also used to model the selected cases, showing good agreement for moderate curvature but not for sharp curvature. An analysis of the driving mechanisms reveals the reason for the difference in the model predictions.

Keywords: Meandering streams, Velocity redistribution, Curvature, Secondary flow, Bed roughness.

1 INTRODUCTION

Meandering rivers are a very common planform throughout the world. Their shape and lateral movement has intrigued scientists and engineers for many centuries (cf. Seminara 2006). Recently, the increased focus on renaturalization projects has led policy makers to consider the partial remeandering of previously trained rivers. However, economic factors such as navigation and man-made infrastructure also set the boundaries for such rivers. To analyze the evolution of meandering river one could use a mathematical model.

Meander models generally consist of three parts i) a hydrodynamic component, ii) a channel morphology component and iii) a channel migration component. The focus of this paper will be primarily on the flow component.

Recently Rüther and Olsen (2007) showed the feasibility of a 3D (three-dimensional) meander model by simulating the 72 hour laboratory experiment by Friedkin (1945). The flow component of their meander model was solved using Reynolds averaged Navier Stokes equations with a k-ε closure (Rodi, 1980) producing a detailed description of the flow.

Spatial and temporal scales of real meandering rivers are several orders of magnitude larger than in Friedkin's experiment, and therefore require the use of reduced hydrodynamic models (e.g. 1D or 2D models) derived from the 3D continuity and momentum equations (see reviews by e.g. Parker & Johannesson, 1989 or Camporeale et al., 2007). 1D models are models in which the system of differential equations is dependent on one coordinate only. Besides being faster, reduced models also have the advantage that they are more insightful than the higher order models as the dominant mechanisms may easily be distilled by considering the model equations. Therefore, there are many advantages for using a reduced model over a 3D model.

The flow through open channel bends is inherently 3D. Reduced hydrodynamic models can only account for 3D flow processes by means of parameterization. An example of such a parameterization is the secondary flow, which is the mo-tion normal to the primary flow direction and is in part responsible for the redistribution of streamwise velocity (Johannesson & Parker, 1989b) and for the shaping of the transverse bed slope (Olesen, 1987), although recent studies show that for large width to depth ratio (B/H) the effect of secondary circulation on the transverse bed slope is of minor importance in comparison to the transverse distribution of the streamwise velocity (see da Silva et al. 2006 and the references therein). Due to the three-dimensional flow structure in curved open channels, processes such as secondary flow require adequate parametrization in reduced models.

Curvature can be expressed by means of geometric parameters, such as depth or width to radius of curvature ratios (H/R or B/R) or the dimensionless Dean number $De = 13(C_f)^{-0.5}(H/R)^{0.5}$ (de Vriend, 1981) which also depends on the friction factor C_f. Blanckaert & de Vriend (2003) introduced another measure of curvature which in addition to geometric parameters also includes information on the flow structure. Their bend parameter $\beta=C_f^{-0.275}(H/R)^{0.5}(\alpha_s+1)^{0.25}$ depends also depends on the dimensionless parameter α_s, which defines the transverse distribution of the depth averaged streamwise velocity. For example $\alpha_s = -1$ and $\alpha_s = 1$ correspond to a potential vortex distribution and a forced vortex distribution respectively (Vardy, 1990). The definition of α_s will be elaborated in the next section. The variable α_s is not constant through the bend. The same holds for the bend parameter β.

Secondary flow models by Rozovskii (1957) and de Vriend (1977), amongst others, consider a streamwise velocity profile which is the same as in a straight channel flow. The secondary flow strength for steady axi-symmetric bend flow ($\partial/\partial t = \partial/\partial s = 0$) follows from a simplified momentum balance in transverse direction, which neglects the interaction between streamwise and transverse velocity, and it is found to be dependent on the friction factor C_f and proportional to H/R. Blanckaert & de Vriend (2003) developed a model which does include the non-linear interaction of the transverse and streamwise velocity profiles. The ratio of the secondary flow strengths for steady axi-symmetric flow predicted by the models of Blanckaert & de Vriend (2003) and de Vriend (1977) is a function of the bend parameter. For mild curvature ($\beta < 0.4$) the models predict almost the same secondary flow strength and for strong curvature ($\beta > 0.8$) the secondary flow strength in the model by de Vriend (1977) is much larger than the model by Blanckaert & de Vriend (2003) (cf. Fig. 10 in Blanckaert & de Vriend 2003). This indicates that secondary flow is overestimated by de Vriend's model for strong curvature as the non-linear interactions between the streamwise and transverse profiles are neglected. The bend parameter, therefore, indicates when including the non-linear interaction between streamwise and transverse profiles is important.

2 NON-LINEAR REDUCED HYDRODYNAMIC MODEL

Blanckaert & de Vriend (2010) derived a non-linear reduced hydrodynamic model, for the domain sketched in Figure 1. U is the bulk velocity and U_s is the depth averaged velocity. The streamwise coordinate is given by s and n represents the transverse coordinate which runs from $-B/2$ to $B/2$. Blanckaert & de Vriend model the streamwise velocity using an exponential distribution in transverse direction: $U_s(s,n) \approx U(1+n/R(s))^{\alpha_s(s)}$. The variables α_s and R define the streamwise velocity pattern through the bend. By taking the transverse gradient of the streamwise velocity and normalizing it by the bulk velocity, a term describing the transverse flow structure is found: $\alpha_s/R \approx (1+n/R)U^{-1}\partial U_s/\partial n$. The model describes the adaptation of the transverse flow structure (α_s/R) as follows:

$$\lambda_w \frac{\partial}{\partial s}\left(\frac{\alpha_s}{R}\right)+\frac{\alpha_s}{R} = F_w, \qquad (1)$$

where the factor λ_w is the flow adaptation length, and the system is subject to the forcing term F_w.

The adaptation length is defined as:

$$\lambda_w = \frac{1}{2}\frac{H}{\psi C_{f0}}\left(1-\frac{m}{12}\frac{\alpha_s+1}{R}\frac{B^2}{R}\right), \qquad (2)$$

where H is the water depth, C_{f0} is the straight channel roughness, ψ represents the increase in roughness due to curvature, turbulence and non-uniformity of the streamwise velocity (Blanckaert & de Vriend 2003; Blanckaert, 2009). $1/R$ is the inverse radius of curvature and B is the channel width. The variable m is a binary integer, which is set to 1 in the non-linear model.

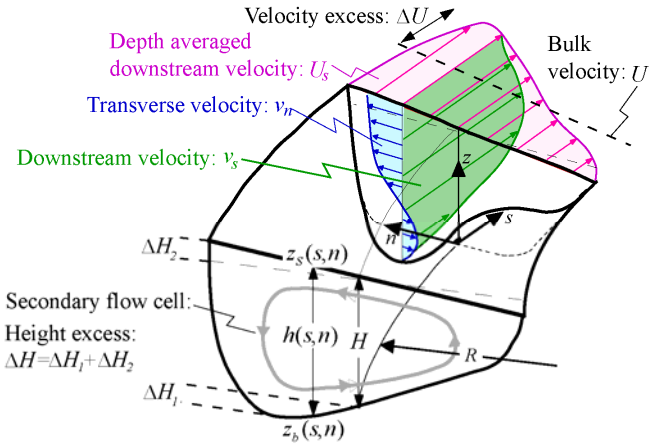

Figure 1. Reference system and variable definition.

The forcing F_w in eq. 1 is defined as:

$$F_w = \frac{1}{2}\frac{S_n^2 Fr^2 + A - 1}{R} \qquad (I)$$

$$-\frac{1}{2}\frac{H}{\psi C_{f0}}\frac{\partial}{\partial s}\left(\frac{1}{R}\right)\left(1-\frac{m}{6}\frac{B^2}{R^2}\right) \qquad (II)$$

$$+\frac{4\chi}{\psi C_{f0}}\frac{H^2}{B^2}\frac{\langle f_s f_n\rangle}{R}\left(1+\frac{m}{12}\frac{(S_n Fr^2 + A + 3)B^2}{R^2}\right) \qquad (III)$$

$$+\frac{m}{24}\frac{H}{\psi C_{f0}}\frac{B^2}{R^2}\frac{\partial}{\partial s}\left(\frac{S_n Fr^2 + A}{R}\right). \qquad (IV)$$

(3)

The first line (I) in eq. (3) relates to the transverse water slope $S_n Fr^2/R$ ($S_n \approx 1$, Fr is the dimensionless Froude number) and the transverse bed slope, which are related in the following way:

$$\left(1+\frac{n}{R}\right)\frac{1}{H}\frac{\partial h}{\partial n} \approx \frac{S_n Fr^2 + A}{R}. \qquad (4)$$

Mechanism (I) is also referred to as topographic steering (Nelson, 1990). The second line (II) in (3) is related to changes in curvature radius, the third (III) relates to the redistribution of the streamwise momentum through secondary flow

$$\langle f_s f_n\rangle / R = U^{-2} H^{-2} \int_{z_b}^{z_s} v_s v_n dz\Big|_{n=0},$$

and the final line (IV) is due to changes in the transverse bed and water level. The constant χ can be derived from the distribution of secondary flow across the width of the channel. Blanckaert & de Vriend (2010) use the value $\chi = 1.5$, because then the model with $m = 0$ reduces to the linear model by Johannesson and Parker (1989b).

The terms $\langle f_s f_n\rangle$ and ψ require closure from the non-linear submodel by Blanckaert & de Vriend (2003). Inertial effects for $\langle f_s f_n\rangle$ and ψ are captured through a linear adaptation equation using the relaxation factor by Johannesson & Parker (1989a).

The choice $m = 0$, $\psi = 1$, and obtaining $\langle f_s f_n\rangle$ and ψ from the linear closure model by de Vriend (1977) results in the linear reduced flow model of Johannesson & Parker (1989b).

3 RESULTS

The non-linear reduced hydrodynamic model by Blanckaert & de Vriend (2010) was validated with two sharply curved flume experiments of piecewise constant curvature radius R performed in Lausanne, Switzerland (Blanckaert, 2009, 2010). The linear model by Johannesson & Parker (1989b) was also validated by means of mildy curved laboratory experiments of piecewise constant curvature radius.

This paper will present a validation of the non-linear hydrodynamic model in more naturally occurring bends. The first case which we consider is a sharply curved multiple bend Kinoshita flume with gradually varying curvature radius R and a flat bed (Abad & Garcia, 2009) following paths which are very similar to natural meandering rivers (Langbein & Leopold, 1966; Parker et al., 1983). The second case concerns a field validation/application to the moderately curved Tollense River. In both cases a comparison will be made with the linear hydrodynamic model.

3.1 *Case A: Kinoshita flume*

Abad & Garcia (2009) performed an experiment in a Kinoshita shaped meander flume (see Figure 2 & Table 1). The smooth boundaries ($C_f \approx 0.005$), flat bed, very narrow cross-section ($B/H = 4$), the average ratios $H/R = 0.19$ and $B/R = 0.75$, and furthermore $\beta \approx 1.17$, which corresponds to a sharp bend, make it a suitable validation case.

Using the linear and non-linear model presented in the previous section the transverse flow structure (is calculated. Figure 3 shows the comparison of the simulated transverse flow structure (α_s/R) compared to the experimental data, showing that the non-linear model succeeds in modeling the flow correctly whereas the linear model overestimates α_s/R which is associated with a too strong secondary circulation.

Table 1. Hydrodynamic and geometric properties of the validation cases. Q is the discharge, H is the mean flow depth, C_{f0} is the friction factor, Fr is the dimensionless Froude number, R_{ap} is the radius of curvature at the bend apex, B/H the average width to depth ratio, B/R the average width to radius ratio, H/R the average depth to radius ratio, $C_{f0}^{-1}H/R$ is a measure of curvature similar to the dimensionless Dean number (de Vriend, 1981), and β is the bend parameter (Blanckaert & de Vriend, 2003).

Case	Q [l/s]	H 10^{-1}[m]	C_{f0} 10^{-3}	Fr 10^{-1}	R_{ap} [m]	B/H	B/R 10^{-1}	H/R	$C_{f0}^{-1}H/R$	β
A	25	1.5	5	2.3	0.67	4	0.75	1.9	38	1.17
B	1500	15	30	0.05	14.2	12.8	0.72	0.6	2	0.5

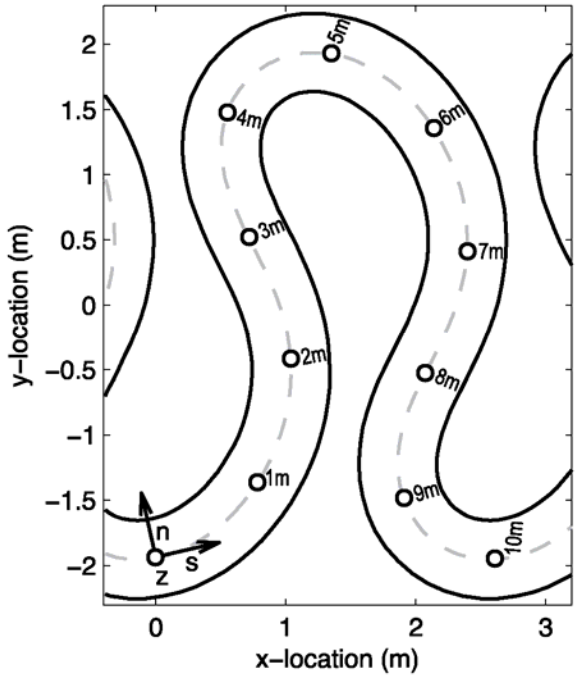

Figure 2. Schematic view of the Kinoshita flume.

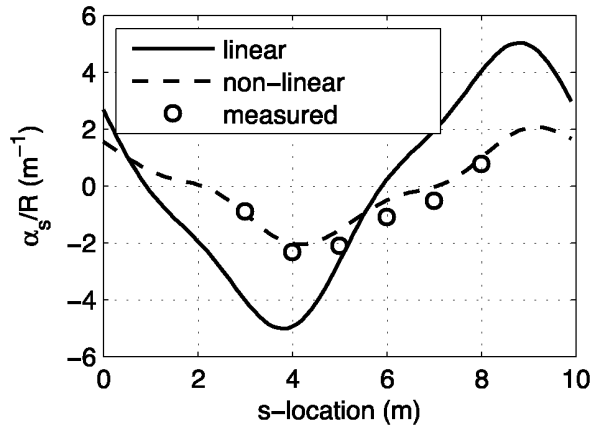

Figure 3. Transverse flow structure for the Kinoshita shaped meander flume calculated by the linear and non-linear hydrodynamic models and compared to measurement data.

3.2 *Case B: Tollense River bend*

Having validated the non-linear model over a smooth flat bed, and noting that Blanckaert and de Vriend (2010) validated the same model for an experimental setup with both a flat and a developed bed, the model will now be subjected to field conditions.

The Leibniz-Institute for Freshwater Ecology and Inland Fisheries (IGB) kindly provided us with field measurement data, obtained by an IGB field team under lead of A. Sukhodolov. The location of the field survey was in a meander bend in the Tollense River. Figure 4 shows a schematic overview of the bend, which varies in width (cf. Figure 5) and is further complicated by horizontal recirculations and river bed vegetation (Schnauder & Sukhodolov, 2010) making it a difficult test case for the non-linear model.

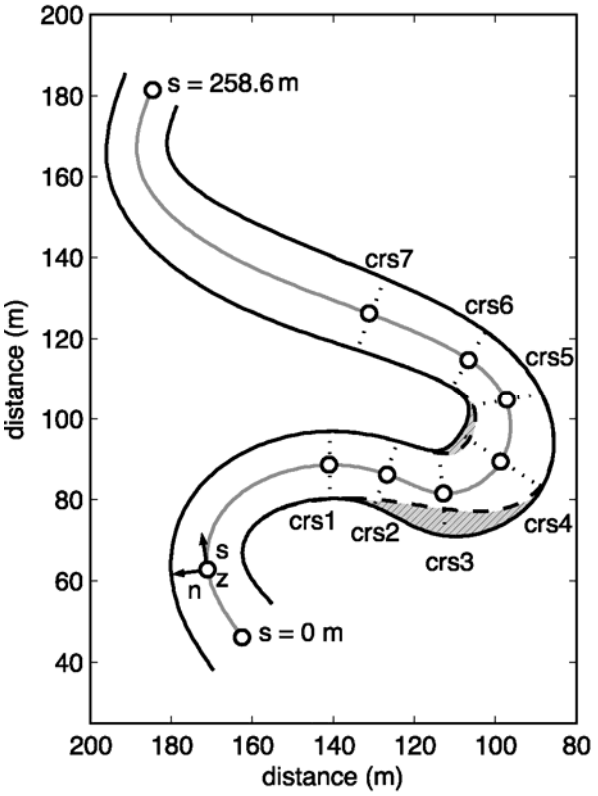

Figure 4. Schematic view on the Tollense River bend. The arched areas indicate separation zones. Measurement data courtesy of Schnauder & Sukhodolov (2010).

Table 1 gives hydrodynamic and geometric properties of the bend. At the bend apex the radius of curvature is $R_{ap} = 14.2$ m. The water depth varies between $H = 1$ m and 2 m through the bend. The average length scale ratios are $H/R = 0.06$, $B/R = 0.72$, $B/H = 12.8$. Furthermore the average friction factor $C_f = 0.03$ which is much rougher than the Kinoshita flume. The average bend parameter $\beta \approx 0.5$ defines a moderate curvature.

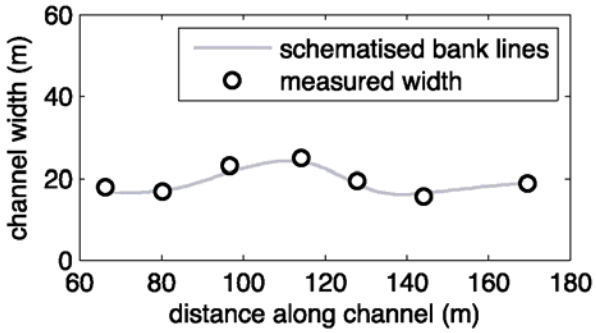

Figure 5. Width along the Tollense River (Schnauder & Sukhodolov, 2010).

The measured bed-level and velocity data is shown in Figure 6. The measured velocities at crs3 and crs4, show that there is a flow in the up-stream direction, indicating the zones of horizontal recirculation. Figure 7 shows the measured width averaged water depth at the cross-sections along the river. The width-averaged streamwise velocity U follows from the conservation of mass $U = Q/(BH)$, where the average discharge Q is

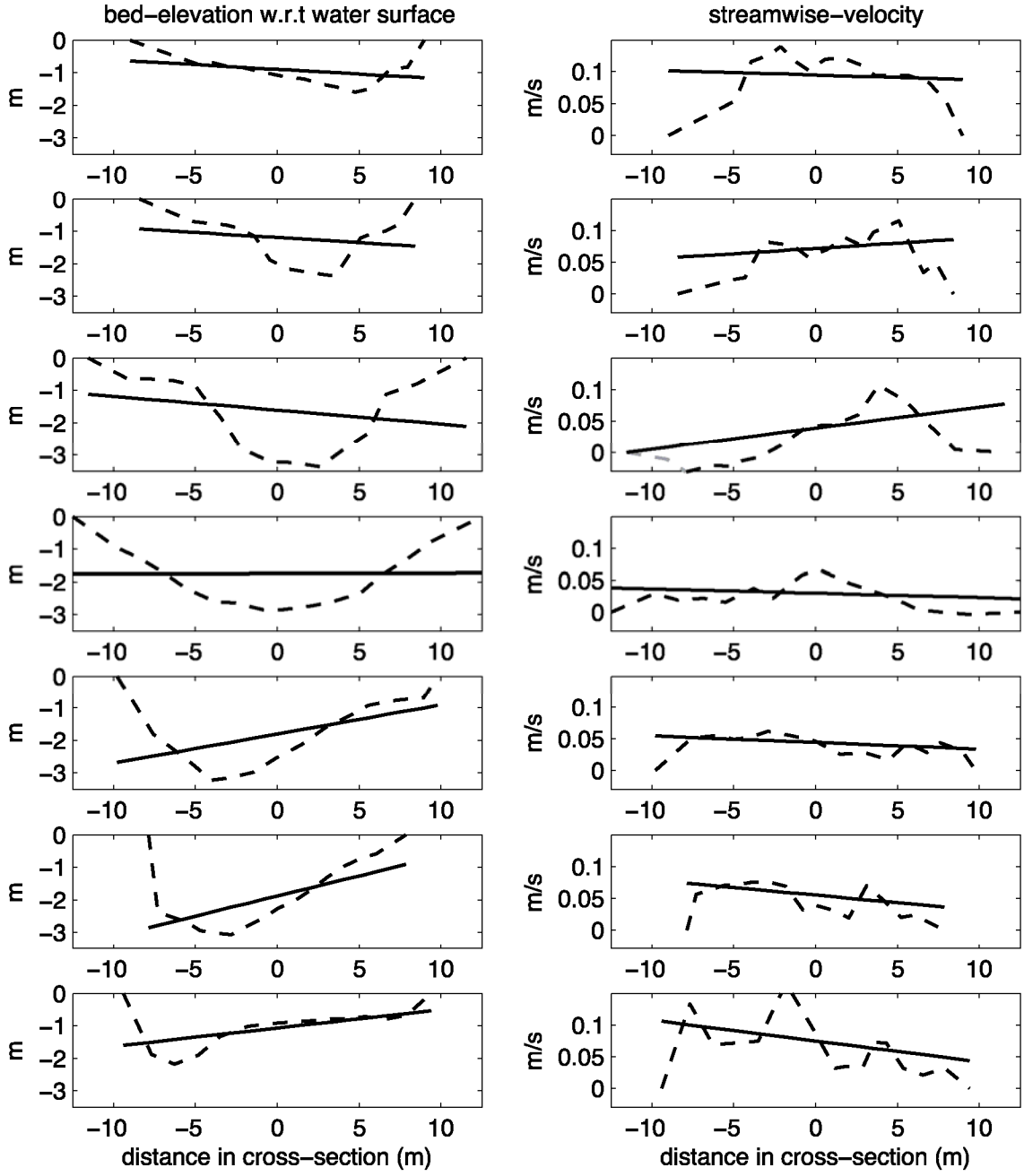

Figure 6. Determining the values of A/R (left) from the bed-elevation with respect to the free water surface and α_s/R (right) from the depth-averaged streamwise velocities through a linear fit (cf. Eq (5)). The rows represent crs1 to crs7 (from top to bottom). Measurement data courtesy of Schnauder & Sukhodolov (2010).

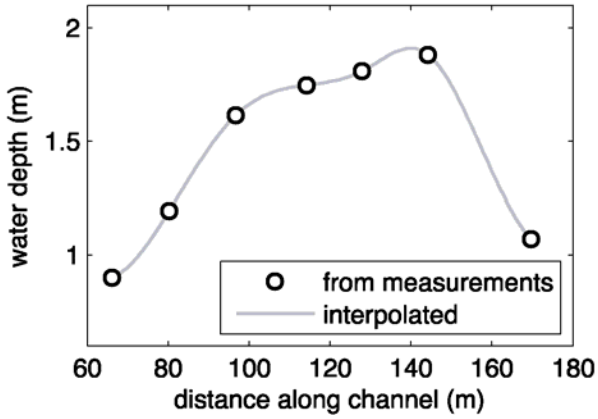

Figure 7. Width averaged depth along the Tollense River bend (Schnauder & Sukhodolov, 2010).

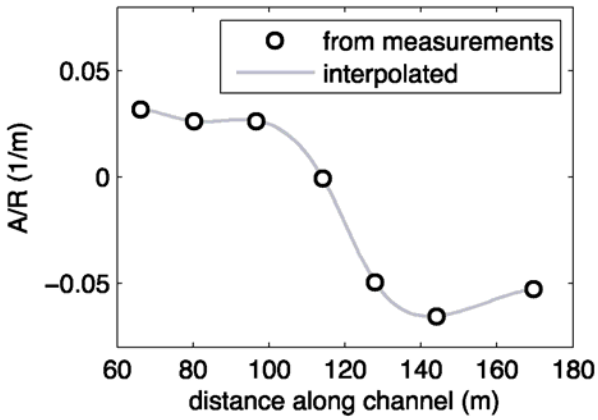

Figure 8. Transverse bed slope derived from the bed level measurements along the Tollense River bend.

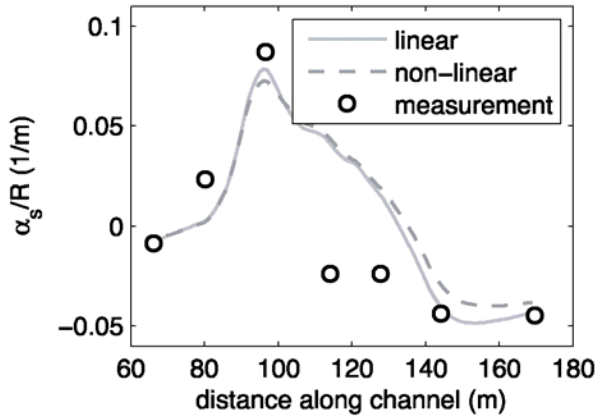

Figure 9. Transverse flow structure along centerline for the Tollense River bend. The values of the transverse flow from the measurements were obtained from the depth-averaged streamwise velocity.

given in Table 1. A/R is approximated through Eq. 4, (where $S_n Fr^2/R \approx 0$), from measurements), by considering the linear fit through the measured depth (see Figure 6). The derived values for A/R are given in Figure 8.

Using the interpolated information from Figures 5, 7 and 8 the transverse flow structure is calculated. Strictly speaking the model in Eq. (1)-(3) is based on a fixed width channel. In the Tollense case the change of the width along the channel is small with respect to the width, which means that the error made neglecting the streamwise change in width $\partial B/\partial s$ is small.

The result for the transverse flow structure is given in Figure 9. The linear and the non-linear model produce almost the same predictions, confirming the classification of moderate curvature. The measured values of the transverse flow structure are determined as:

$$\alpha_s/R \approx (1+n/R)U^{-1}\partial U_s/\partial n \approx U^{-1}\partial U_s/\partial n \qquad (5)$$

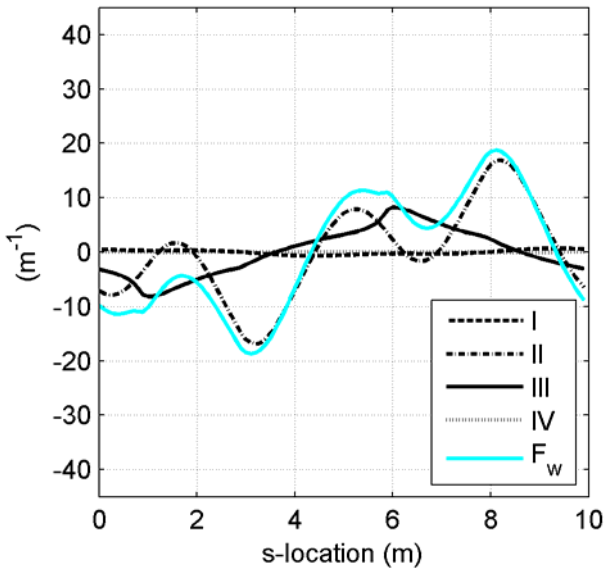

Figure 10. Relative and total contributions of the forcing terms in the non-linear hydrodynamic for the Kinoshita shaped meander flume. The legend refers to eq. (3).

by the linear fit of the streamwise velocities given in Figure 6. The values of the transverse flow structure interpolated from the measurements are not correctly predicted by the model along the full bend. Between crs1 and crs3 the predictions show the correct trend. In the middle reach crs3-crs5 where the channel widening takes place the predicted values show a deviation from the values obtained from measurements. The final section crs5 to crs7 show good agreement again. Locally the non-linear model predictions for the Tollense River deviate from the measured data. Globally (from bend entrance to bend exit), however, the predicted flow pattern agrees well with the measured data.

4 DISCUSSION

In the previous section, the non-linear model predictions shows good agreement to the global flow pattern obtained from a sharp curvature laboratory experiment as well as from a moderate curvature field experiment. In this section the results will be discussed by analyzing the dominant mechanisms for velocity redistribution and comparison to a linear model.

4.1 *Sharp curvature*

For the sharply curved Kinoshita flume we shall distinguish between the processes that are responsible for the redistribution of streamwise velocity by considering the mechanisms provided in eq. (3). Figure 10 shows the relative contributions of the total forcing F_w for the Kinoshita flume. The forcing F_w is dominated by

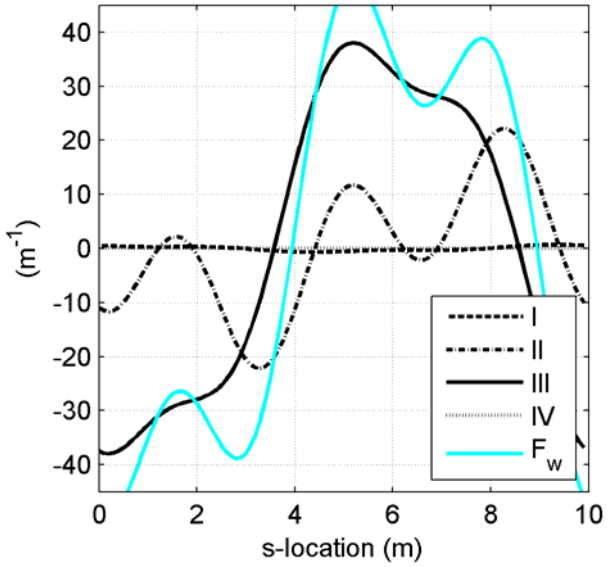

Figure 11. Relative and total contributions of the forcing terms in the linear hydrodynamic for the Kinoshita shaped meander flume. The legend refers to eq. (3).

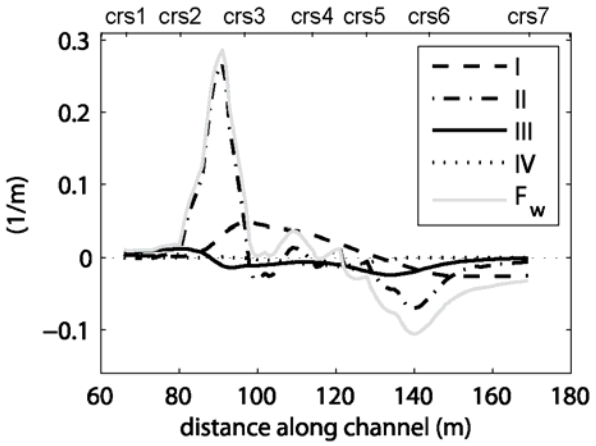

Figure 12. Relative and total contributions of the forcing terms in the non-linear hydrodynamic simulation for the Tollense River bend. The legend refers to eq. (3).

the change in curvature radius (II), except locally around s = 1 m and s = 7 m, where secondary flow (III) has a substantial contribution. Therefore, the change in curvature radius is the most important mechanism for velocity redistribution.

For comparison, Figure 11 shows the importance of the forcing mechanisms in the linear model when simulating the Kinoshita flume. The linear model indicates that the secondary flow mechanism (III) is the dominant mechanism for velocity redistribution, except between $s = 3$ m to 4 m and between $s = 8$ m to 9 m where the change in curvature radius (II) is the most important mechanism. From this we may conclude that the linear model fails to reproduce the experimental data (cf. Figure 3), because it overestimates the effect of secondary flow. The linear model erroneously identifies the flow redistribution due to secondary flow (III) as the dominant mechanism for streamwise flow redistribution whereas the non-linear model shows that the change in curvature radius (II) is really the dominant mechanism.

4.2 *Moderate curvature*

The second case is a moderate curvature bend in the Tollense River in the field. As shown in Figure 9, the global flow field was well captured by both the linear and the non-linear model. Locally, between crs3 and crs5 there are differences. We think the main reasons for the differences between the model predictions and the measured data are: The effect of horizontal recirculations and river bed vegetation are not included in the model; and the model considers only one degree of freedom for the transverse bed levels which is clearly not sufficient as can be seen in Figure 6. Nevertheless, the global behavior shows good agreement, and we will therefore continue by analyzing the dominant factors

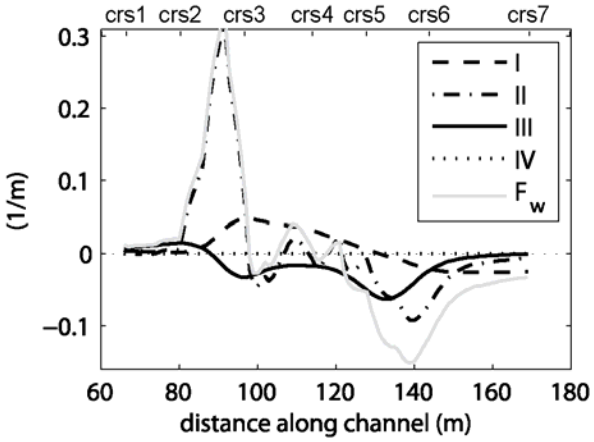

Figure 13. Relative and total contributions of the forcing terms in the linear hydrodynamic simulation for the Tollense River bend. The legend refers to eq. (3).

affecting the global velocity redistribution in the Tollense River bend.

The forcing mechanisms as calculated by the non-linear model are shown in Figure 12. The dominant forcing between crs1 and crs2 is due to secondary flow (III). Between crs2 and crs3 the change in curvature radius (II) is the dominant mechanism for flow redistribution. Between crs3 and crs5 redistribution through topographic steering (I) is found to be the dominant mechanism. The change in curvature radius (II) is the most important mechanism between crs5 and crs6 and topographic steering (I) dominates the flow redistribution in the final section crs6 to

crs7. Velocity redistribution in the Tollense River is caused by a combination of mechanisms namely by topographic steering (I), change in curvature radius (II) and by secondary flow (III).

Contrary to the flat bed Kinoshita flume the Tollense River shows a pronounced bed topography (cf. Figure 6) which shows that for field conditions topographic steering (I) becomes an important mechanism for velocity redistribution.

Comparison to a linear model shows almost the same contributions (cf. Figure 13). The sole difference is between crs4 and crs5 where the secondary flow mechanism is dominant. The reason that both the linear and the non-linear model give similar results is because of the high roughness which causes a lower secondary flow contribution (cf. eq. (3), line (III)) and consequently less difference between the linear and non-linear model.

5 CONCLUSION

This paper showed the validation of the non-linear hydrodynamic model by Blanckaert and de Vriend (2010) for two naturally shaped bend flows. For the sharply curved Kinoshita shaped meander flume over a smooth flat bed, the non-linear model compared very well to the measurements, whereas the linear model did not. The main reason that the linear model was unable to reproduce the measurements was due to the overestimation of the role of secondary flow (III). For the sharply curved Kinoshita flume experiment, the change in curvature radius (II) was the dominant forcing term for the redistribution of streamwise momentum.

For the moderately curved bend of the Tollense River, both the linear and the non-linear model showed a similar prediction of the overall flow structure, comparing well with the measured data. Locally there were differences which could be caused by the effect of the horizontal recirculations, river bed vegetation, and the model's lack of resolution in transverse direction. An analysis of the driving mechanisms of the global velocity redistribution showed that it was caused by topographic steering (I), change in curvature radius (II) and by secondary flow (III).

Based on the two selected cases it is shown that the non-linear model performs well in both moderate and sharp curvature. The linear model is suitable for moderately curved bends, but fails to model sharply curved bends, as it overestimates the effect of secondary flow. In sharply curved bends it is found that the change in curvature radius is the dominant mechanism for velocity redistribution, yet the linear model erroneously identifies secondary flow to be the dominant mechanism.

ACKNOWLEDGEMENTS

We would like to thank Jorge Abad for the Kinoshita experiment data. We thank Ingo Schnauder and Alex Sukhodolov for the Tollense field data (Funding for the field survey was provided by DFG project SU405/3-1 and NWO-DFG project DN66-149). The Dutch Technology Foundation (STW), applied science division of NWO is gratefully acknowledged for the research grant DCB.7780. The support of Deltares is also gratefully acknowledged.

REFERENCES

Abad, J. D., Garcia, M. H., 2009. Experiments in a high-amplitude Kinoshita meandering channel: 1. Implications of bend orientation on mean and turbulent flow structure. Water Resour. Res., 45. W02401; DOI:10.1029/2008WR007016.

Blanckaert, K. 2009. Saturation of curvature-induced secondary flow, energy losses, and turbulence in sharp open-channel bends: Laboratory experiments, analysis, and modeling. J. Geophys. Res., 114, F03015, DOI:10.1029/2008JF001137.

Blanckaert, K. 2010. "Laboratory experiments on straight and sharply curved open-channel flows. Experimental techniques, data treatment and selected results". (submitted for publication to Water Resources Research, AGU)

Blanckaert, K., de Vriend, H. J. 2003. Nonlinear Modeling of Mean Flow Redistribution in Curved Open Channels. Water Resources Research, 39(12); DOI:10.1029/2003WR002068.

Blanckaert, K., de Vriend, H. J. 2010. Meander dynamics: a 1D flow model without curvature restrictions. submitted to Journal of Geophysical Research.

Camporeale, C., Perona, P., Porporato, A., Ridolfi, L., 2007. Hierarchy of models for meandering rivers and related morphodynamic processes. Reviews of Geophysics, 45(1). DOI:10.1029/2005RG000185.

da Silva, A. M. F., El-Tahawy, T., Tape, W. D. 2006. Variation of flow pattern with sinuousity in sine-generated meandering streams. J. Hydraul. Eng., 132(10), 1003-1014.

de Vriend, H. J. 1977. A mathematical model of steady flow in curved shallow channels. J. Hydr. Res., 15(1):37-54, 1977.

de Vriend, H. J., 1981. Velocity redistribution in curved rectangular channels, J. Fluid Mech., 107, 423– 439.

Friedkin, J. F. 1945. A Laboratory Study of the Meandering of Alluvial Rivers. Technical report, U.S. Waterways Experiment Station, Mississippi.

Johannesson H., Parker, G. 1989a. Secondary flow in mildly sinuous channel. J. Hydr. Engng, 115(3):289-308.

Johannesson H., Parker, G. 1989b. Velocity redistribution in meandering rivers. J. Hydr. Engng, 115(8):1019-1039.

Langbein, W. B. and Leopold, L. B., 1966. River meanders: theory of minimum variance. Technical report, USGS 561 Professional Paper 422-H

Nelson, J. E., 1990. The initial instability and finite-amplitude stability of alternate bars in straight channels. Earth Science Reviews, 29:97–115.

Parker, G., Diplas, P., Akiyama, J., 1983. Meander bends of high amplitude (channel migration). J. Hydr. Engng, 109(10):1323–1337.

Parker, G., Johannesson, H., 1989. Observations on several recent theories of resonance and overdeepening in meandering channels. In Ikeda, S. and Parker, G., editors, River Meandering, volume 12, pages 379–415. AGU. ISBN 584 0-87590-316-9.

Rodi, W., 1980. Turbulence Models and their Application in Hydraulics. IAHR State-of-the-art Publication, Monograph Series, third ed. A.A. Balkema, Rotterdam.

Rozovskii, I. L. 1957. Flow of Water in Bends of Open Channels, Acad. of Sci. of the Ukr., Kiev, 1957. (English translation, Isr. Program for Sci. Transl., Jerusalem, 1961.)

Rüther, N., Olsen, N. R. B. 2007. Modelling free-forming meander evolution in a laboratory channel using three-dimensional computational fluid dynamics. Geomorphology, 89(3-4):308—319;

Seminara, G. 2006. Meanders. J. Fluid Mech. 554:271-297; DOI :10.1017/S0022112006008925.

Schnauder, I., Sukhodolov, A. N., 2010. Three-dimensional flow structure in a meander bend with aquatic macrophytes. in prep. for subm. to Earth Surface Processes and Landforms.

Vardy, A., 1990. Fluid Principles. McGraw-Hill